

See discussions, stats, and author profiles for this publication at: <https://www.researchgate.net/publication/256649483>

# Degradation of high-molar-mass hyaluronan and characterization fragments

ARTICLE in BIOMACROMOLECULES · JANUARY 2007

Impact Factor: 5.75

---

READS

31

7 AUTHORS, INCLUDING:



**Grigorij Kogan**

European Commission

**117** PUBLICATIONS **2,608** CITATIONS

SEE PROFILE



**Raniero Mendichi**

Italian National Research Council

**119** PUBLICATIONS **2,333** CITATIONS

SEE PROFILE



**Jozef Rychlý**

Slovak Academy of Sciences

**147** PUBLICATIONS **1,229** CITATIONS

SEE PROFILE



**Peter Gemeiner**

Slovak Academy of Sciences

**259** PUBLICATIONS **3,341** CITATIONS

SEE PROFILE

## Degradation of High-Molar-Mass Hyaluronan and Characterization of Fragments

L. Šoltés,<sup>†</sup> G. Kogan,<sup>\*,‡,§</sup> M. Stankovská,<sup>†,○</sup> R. Mendichi,<sup>§</sup> J. Rychlý,<sup>||</sup> J. Schiller,<sup>⊥</sup> and P. Gemeiner<sup>‡</sup>

*Institute of Experimental Pharmacology, Slovak Academy of Sciences, SK-84104 Bratislava, Slovakia, Institute of Chemistry, Slovak Academy of Sciences, SK-84538 Bratislava, Slovakia, Istituto per lo Studio delle Macromolecole, Consiglio Nazionale delle Ricerche, I-20133 Milano, Italy, Polymer Institute, Slovak Academy of Sciences, SK-84236 Bratislava, Slovakia, and Medical Faculty, Institute of Medical Physics and Biophysics, University of Leipzig, D-04107 Leipzig, Germany*

*Received March 19, 2007; Revised Manuscript Received June 19, 2007*

A sample of high-molar mass hyaluronan was oxidized by seven oxidative systems involving hydrogen peroxide, cupric chloride, ascorbic acid, and sodium hypochlorite in different concentrations and combinations. The process of the oxidative degradation of hyaluronan was monitored by rotational viscometry, while the fragments produced were investigated by size-exclusion chromatography, matrix-assisted laser desorption/ionization–time-of-flight mass spectrometry, and non-isothermal chemiluminometry. The results obtained imply that the degradation of hyaluronan by these oxidative systems, some of which resemble the chemical combinations present *in vivo* in the inflamed joint, proceeds predominantly via hydroxyl radicals. The hyaluronan fragmentation occurred randomly and produced species with rather narrow and unimodal distribution of molar mass. Oxidative degradation not only reduces the molecular size of hyaluronan but also modifies its component monosaccharides, generating polymer fragments that may have properties substantially different from those of the original macromolecule.

### Introduction

Hyaluronan synthases (HAS1, HAS2, and HAS3), the enzymes localized in the vertebrate cells within a putative organelle called the hyaluronasome, synthesize hyaluronan (HA) with high molar mass. HAS1 and HAS2 produce relatively large forms of HA ( $2 \times 10^5$ – $2 \times 10^6$  Da), while HAS3 produces polymers only half that size ( $10^5$ – $10^6$  Da).<sup>1</sup>

In the initial phases of the commercial production of high-molar-mass HA, various tissues obtained from phylogenetically higher organisms, for example, rooster combs, were utilized. For example, the Swedish company Pharmacia used to occupy a dominant position in the market for HA products designed for ophthalmologic surgery purposes. Its product, Healon, has long been the only appropriate material applied to so-called viscosurgical operations.<sup>2</sup>

The prepared batches of Healon as well as other HA preparations produced from vertebrate tissues or by bacterial fermentation of suitable strains, for example, *Streptococcus*, were subjected to molecular characterization preferentially by means of size-exclusion chromatography (SEC). Calibration of the SEC columns, which has been initially performed using a set of defined pullulan molecular standards, was increasingly

replaced by the application of HA fragments with different molar masses. These were prepared by means of degradation/depolymerization of high-molar-mass HA using the enzyme hyaluronidase or by applying physical and/or chemical methods such as acidic or basic hydrolyses, thermal degradation, and/or exposure to  $\gamma$ -irradiation.<sup>3,4</sup>

Increased interest in HA preparations with smaller molar masses has occurred recently because of the observation that these fragments have size-specific functions. While high-molar-mass HA possesses anti-angiogenic, anti-inflammatory, and immunosuppressive properties,<sup>5–7</sup> intermediate-sized HA fragments act predominantly in an opposite manner, that is, they are angiogenic, pro-inflammatory, and immunostimulating.<sup>8,9</sup> Concurrently, HA preparations with a precisely defined narrow molar mass distribution have been recently introduced to the market.<sup>10</sup>

In the living organism, the biosynthesized high-molar-mass HA plays several roles. For example, free, nonassociated HA in synovial fluid (SF) confers its unique viscoelastic properties required for maintaining proper functioning of the joints. Hyaluronan associated with certain glycosaminoglycans and proteins has an important function in organizing the extracellular matrix (ECM) as well as in binding and concentrating certain growth factors.<sup>11</sup>

An adult person weighing 70 kg has ca. 15 g of HA in the body. About one-third of this amount turns over daily. The half-life of HA is a few minutes in blood, several hours in SF, 1 to 2 days in the epidermal compartment of skin, and less than 3 weeks in cartilage. Although such relatively fast catabolism of HA in the organism is controlled by hyaluronidases, some tissues such as SF lack these enzymes, and rapid catabolism of HA may have a different mechanism. Fast HA turnover in the joints of healthy individuals may be attributed to the oxidative/degradative action of reactive oxygen species (ROS), among

\* Corresponding author. Dr. Grigorij Kogan, Institute of Chemistry, Slovak Academy of Sciences, Dúbravská cesta 9, SK-84538 Bratislava, Slovakia. Fax: +421-2-5941-0222. E-mail: grigorij.kogan@savba.sk.

<sup>†</sup> Institute of Experimental Pharmacology, Slovak Academy of Sciences.

<sup>‡</sup> Institute of Chemistry, Slovak Academy of Sciences.

<sup>§</sup> Consiglio Nazionale delle Ricerche.

<sup>||</sup> Polymer Institute, Slovak Academy of Sciences.

<sup>⊥</sup> University of Leipzig.

<sup>○</sup> Present address: Directorate General Research, European Commission, B-1050, Brussels, Belgium.

<sup>○</sup> Present address: Food Research Institute, SK-82475 Bratislava, Slovakia.

others, generated by the catalytic effect of transition metal ions on the auto-oxidation of ascorbate.<sup>12</sup> The detection of the low-molar-mass HA fragments in the joints of patients affected by rheumatoid arthritis (RA) can be explained by enhanced ROS production in the inflamed joint by infiltrating leukocytes.<sup>13</sup> It is exactly the latter phenomenon or, more precisely, intermediate- and/or small-sized HA fragments generated by it, that constitute the subject of our current research. HA fragments prepared *in vitro* via procedures similar to those occurring under physiological or pathophysiological conditions would be more suitable for *in vivo* studies than HA fragments generated by the physical and/or chemical procedures.

Here, we present new results on HA degradation using oxidative systems containing ascorbic acid, report characterization of the obtained fragments, and compare the new data with our previously published results. The HA fragments were prepared by using reagents that participate in the catabolism of high-molar-mass HA in the healthy and in the inflamed joint. The molar mass distribution (MMD) of the resulting polymer fragments was evaluated by a multi-angle light scattering (MALS) detector connected on-line to a SEC system. Methods of non-isothermal chemiluminescence along with matrix-assisted laser desorption ionization–time-of-flight mass spectrometry (MALDI-TOF MS) were applied to the polymer fragments.

## Experimental Procedures

**Intact HA Samples.** The two samples of high-molar-mass HA were provided by Dr. K. Thacker from Lifecore Biomedical Inc., Chaska, MN (sample coded LIFECORE P9710-2;  $M_w = 1215$  kDa,  $M_w/M_n = 1.79$ ) and by CPN Ltd., Ústí nad Orlicí, Czech Republic (sample coded CPN;  $M_w = 659.4$  kDa;  $M_w/M_n = 1.88$ ).<sup>14</sup> In the LIFECORE P9710-2 sample, the presence of 13 ppm of iron and 4 ppm of copper ions has been acknowledged ["Certificate of Analysis" (Lifecore Biomedical Inc.)].

**Chemicals.** NaCl and  $\text{CuCl}_2 \cdot 2\text{H}_2\text{O}$ , analytical purity grade, were from Slavus Ltd., Bratislava, Slovakia. Ascorbic acid and methanol were from Merck KGaA, Darmstadt, Germany. Ethanol ( $\approx 96\%$ , v/v) and an aqueous solution of  $\text{H}_2\text{O}_2$  ( $\approx 30\%$ ) were purchased from Chemapol, Prague, Czech Republic. Aqueous solution of NaOCl ( $\approx 1$  M, containing 6–14% active chlorine) was the product of Riedel de Haen AG, Seelze, Germany. Bovine testicular hyaluronidase with an activity of 400–1000 U/mg was purchased as a lyophilized powder from Sigma-Aldrich Chemical Co. (St. Louis, MO) and used without further purification. The MALDI-TOF matrix, 2,5-dihydroxybenzoic acid (DHB), obtained from Fluka, was also used as supplied. Water applied for HA degradation was of redistilled deionized quality grade.

**Stock/Working Solutions.** The stock hydrogen peroxide solution was prepared by dissolving NaCl in commercial  $\text{H}_2\text{O}_2$  to a salt concentration of 0.15 M. The working  $\text{H}_2\text{O}_2$  solutions were prepared immediately before the experiment by appropriate dilution of hydrogen peroxide stock solution with 0.15 M NaCl. The stock  $\text{CuCl}_2$  solution and that of ascorbic acid were also prepared freshly in 0.15 M NaCl. The aqueous solutions of sodium hypochlorite were prepared by dilution of commercial NaOCl solution in redistilled deionized water. Dissociation of NaOCl at neutral pH results in nearly equimolar concentrations of non-dissociated acid (HOCl) and the hypochlorite anion ( $^-\text{OCl}$ ) because of the value of  $\text{p}K_a$  7.53.<sup>15</sup> For this reason as well as for current convention, we used a simplified designation HOCl instead of a more precise  $\text{HOCl}/^-\text{OCl}$ . The actual concentrations of the working aqueous  $\text{H}_2\text{O}_2$  and HOCl solutions were determined spectrophotometrically.<sup>16,17</sup>

**Rotational Viscometry/Preparation of HA Fragments.** In order to investigate rheological properties, 20.0 mg of high-molar-mass HA sample (LIFECORE P9710-2 or CPN) was dissolved in 0.15 M NaCl overnight in the dark at room temperature in two steps: first, 4.0 mL solvent was added, and second, the next 4.0 mL portion of the solvent

was added after 6 h. The dynamic viscosity ( $\eta$ ) values of the native HA samples was 12.05 mPa·s (LIFECORE P9710-2) and 5.80 mPa·s (CPN).

A similar two-step procedure was applied in dissolving the HA sample (LIFECORE P9710-2). However, the second solvent portion was smaller than 4.0 mL (usually from 3.20 to 3.90 mL). The remaining volume was brought to a total of 8.0 mL by gradually adding reagents. In the case of the  $\text{CuCl}_2$  solution, it was admixed to the HA solution 9 min before the application of other reagents:  $\text{H}_2\text{O}_2$  alone or with ascorbic acid; the latter was added directly prior to the application of  $\text{H}_2\text{O}_2$ . When using HOCl solution, it was used as a strong oxidant substituting for  $\text{H}_2\text{O}_2$  and applied at a corresponding time. Altogether, seven different oxidative systems involving different combinations and concentrations of reagents were utilized: (a) 882 mM  $\text{H}_2\text{O}_2$  (HP882); (b) 1.25  $\mu\text{M}$   $\text{CuCl}_2$  and 55 mM  $\text{H}_2\text{O}_2$  (CU1.25-HP55); (c) 0.1  $\mu\text{M}$   $\text{CuCl}_2$ , 100  $\mu\text{M}$  ascorbic acid, and 100  $\mu\text{M}$   $\text{H}_2\text{O}_2$  (CU0.1-AA100-HP0.1); (d) 10 mM NaOCl (HOCL10); (e) 0.1  $\mu\text{M}$   $\text{CuCl}_2$ , 100  $\mu\text{M}$  ascorbic acid, and 10 mM NaOCl (CU0.1-AA100-HOCL10); (f) 0.1  $\mu\text{M}$   $\text{CuCl}_2$ , 100  $\mu\text{M}$  ascorbic acid, and 2 mM NaOCl (CU0.1-AA100-HOCL2); and (g) 0.1  $\mu\text{M}$   $\text{CuCl}_2$  and 100  $\mu\text{M}$  ascorbic acid (CU0.1+AA100). The codes given in parentheses symbolize the designation of a polymer fragment prepared using the corresponding oxidative system.

The resulting solutions (8.0 mL) were immediately transferred to the Teflon cup reservoir of the rotational viscometer. Recordings of the viscometer output parameters were started 2 min after onset of the experiment. The changes of dynamic viscosity and torque were monitored at  $25 \pm 0.1$  °C by using a digital rotational viscometer Brookfield DV-II+ PRO (Brookfield Engineering Labs., Inc., Middleboro, MA) equipped with a cup-spindle pair built of Teflon at our laboratory.<sup>18</sup> At the spindle rotational speed of 180 rpm, the shear rate was 237.6  $\text{s}^{-1}$ . The LIFECORE P9710-2 sample degradation was monitored in 3 min intervals for up to 5 h or until the nominal  $\eta$  value 5.8 mPa·s was reached. Within the monitored interval of the  $\eta$  values, the torque ranged between 72 and 36%.

To assay the reaction products, the reservoir content was poured into 20 mL of ethanol, which led to the precipitation of the polymer. On the following day, the polymer precipitate was washed with 20 mL of ethanol, centrifuged, and dried in a desiccator. The yields of the recovered polymer fragments ranged between 15 and 17 mg, that is, the recovery rate was between 75 and 85%. The pellet prepared from the dried polymer obtained from the degradative systems involving hydrogen peroxide was very firm. However, the pellet prepared from the dried polymer obtained in the presence of sodium hypochlorite was brittle, and the odor of chlorine was detected even after the precipitation of the degraded sample.

**SEC-MALS Analysis.** Samples degraded by using the above-listed oxidative systems were molecularly characterized by the SEC-MALS method. Prior to analysis, the degraded sample was dissolved overnight to the desired sample concentration in 0.15 M NaCl. On the following morning, the sample solution was diluted to the required concentration by adding additional 0.15 M NaCl. Prior to analysis, each sample was clarified by filtration through a 0.45  $\mu\text{m}$  Nylon filter (Millipore Corporation, Bedford, MA). The MMD analysis of the samples was performed by using a modular multi-detector SEC system. The SEC system consisted of an Alliance 2690 separation module from Waters (Milford, MA) equipped with two on-line detectors, namely, with a MALS Dawn DSP-F photometer from Wyatt Technology (Santa Barbara, CA) and a DRI 410 differential refractometer from Waters. The latter detector was used to determine the biopolymer concentration in the effluent. The setup of this multi-detector SEC system was serial in the following order: Alliance-MALS-DRI. It is well known that an on-line MALS detector coupled to a concentration detector facilitates the determination of the true molar mass value ( $M$ ) and the size, that is, the root-mean-square radius ( $\langle s^2 \rangle^{1/2}$ ), hereafter referred to as the radius of gyration ( $R_g$ ), of each fraction of the eluted polymer.

The experimental methodology for a reliable use of the MALS photometer has been described in detail.<sup>19–21</sup> Briefly, the MALS

photometer uses a vertically polarized He–Ne laser at  $\lambda = 632.8$  nm and simultaneously measures the intensity of the scattered light at 18 fixed angular locations ranging in aqueous solutions from  $14.5^\circ$  to  $158.3^\circ$  by means of an array of photodiodes. The MALS calibration constant is calculated using toluene as a standard assuming a Rayleigh factor  $R(\theta) = 1.406 \times 10^{-5} \text{ cm}^{-1}$ . Normalization of the photodiodes was performed by measuring the scattering intensity in the mobile phase of bovine serum albumin (BSA;  $M \approx 67$  kDa,  $R_g = 2.9$  nm), a globular protein that is assumed to act as an isotropic scatterer. The specific refractive index increment,  $dn/dc$ , used was  $0.15 \text{ mL/g}$ .<sup>20</sup>

The experimental conditions of the SEC-MALS system were as follows: two stainless steel columns (both  $7.8 \text{ mm} \times 30 \text{ cm}$ ) were connected in series with a guard precolumn; packings were TSKgel of PW type (G6000 and G5000;  $17 \mu\text{m}$  particle size; Tosoh Bioscience, Stuttgart, Germany); separation temperature =  $35^\circ\text{C}$ ; vacuum degassed mobile phase aqueous  $0.15 \text{ M NaCl}$  solution; sample injection volume =  $150 \mu\text{L}$ ; the biopolymer concentration in the injected samples ranged from  $0.1$  to  $2 \text{ mg/mL}$ , depending on the sample molar mass; and the mobile phase flow rate =  $0.4 \text{ mL/min}$ . The data acquisition and analysis softwares used were EMPOWER PRO from Waters and ASTRA 4.73 from Wyatt Technology.

**Non-Isothermal Chemiluminometry.** Chemiluminescence measurements were performed with a photon-counting instrument Lumipol 3 manufactured at the Polymer Institute of the Slovak Academy of Sciences. The sample was placed on an aluminum pan in the sample compartment. The gas flow (pure oxygen or nitrogen) through the sample cell was  $3.0 \text{ L/h}$ . The temperature in the sample compartment of the apparatus was raised from  $40$  to  $220^\circ\text{C}$  with a linear gradient of  $2.5^\circ\text{C/min}$ . The signal of the photocathode was recorded at  $10 \text{ s}$  intervals. The amount of samples used for each measurement ranged from  $1.0$  to  $1.6 \text{ mg}$ .

**MALDI-TOF MS Analysis.** The samples investigated were dissolved in redistilled deionized water to a final concentration of  $5 \text{ mg/mL}$  and subsequently digested by hyaluronidase ( $1 \text{ mg/mL}$  final concentration) at  $37^\circ\text{C}$  for  $24 \text{ h}$ . Afterward, aliquots of all digests were diluted  $1:1$  (v/v) with the matrix ( $0.5 \text{ M DHB}$  in methanol) and placed onto a mate steel target for MALDI-TOF analysis. DHB is the matrix of choice for the analysis of comparably small molecules because this matrix provides only relatively weak signals.<sup>22,23</sup> Subsequently, the solvent was rapidly evaporated using a heat gun to achieve homogeneous crystallization between the matrix and the analyte.

All MALDI-TOF MS measurements were carried out using an Autoflex MALDI-TOF mass spectrometer (Bruker Daltonics, Leipzig, Germany). This instrument uses a pulsed  $\text{N}_2$  laser operating with an excitation wavelength of  $337 \text{ nm}$ . To improve the resolution, all measurements were carried out in the reflector mode under delayed extraction conditions. More details of such measurements have been provided in a recent publication.<sup>24</sup> Both positive and negative ion spectra were recorded. The negative ion spectra were less complex and provided enhanced sensitivity.<sup>23</sup>

## Results

**Rotational Viscometry.** Figure 1 demonstrates the decrease of HA solution viscosity during sample treatment, applying the seven different oxidative systems. Obviously, in all cases, the viscosity of the solution dropped rather quickly. Solution of the LIFECORE P9710-2 sample ( $2.5 \text{ mg/mL}$ ) upon application of the highly concentrated aqueous hydrogen peroxide ( $882 \text{ mM} \equiv 3\%$ ) showed a rapid decline of dynamic viscosity value to  $5.8 \text{ mPa}\cdot\text{s}$ , which lasted about  $165 \text{ min}$  (curve a in Figure 1). Reduction of  $\text{H}_2\text{O}_2$  concentration from  $882 \text{ mM}$  to  $100 \mu\text{M}$  resulted in the absence of any significant decrease of sample dynamic viscosity during the entire  $300 \text{ min}$  monitoring period (data not shown), whereas the addition of a submicromolar amount of  $\text{Cu(II)}$  (namely,  $0.1 \mu\text{M CuCl}_2$ ) along with  $100 \mu\text{M}$

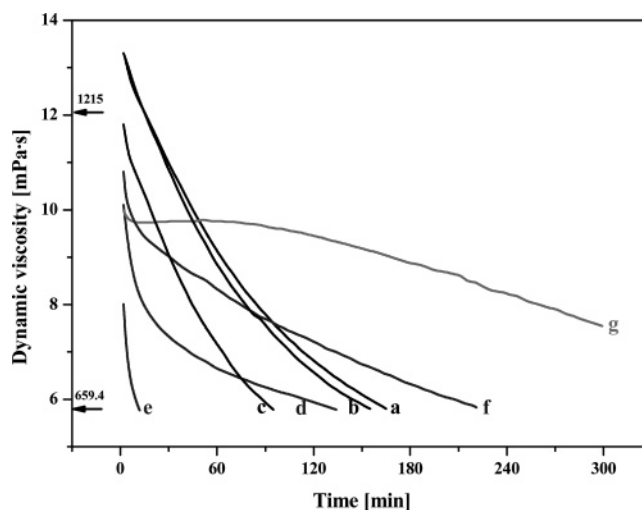


**Figure 1.** Dynamic viscosity vs time profile of a 0.25% (w/v) solution of LIFECORE P9710-2 sample incubated with the following oxidative systems: (a)  $882 \text{ mM H}_2\text{O}_2$ ; (b)  $1.25 \mu\text{M CuCl}_2$  and  $55 \text{ mM H}_2\text{O}_2$ ; (c)  $0.1 \mu\text{M CuCl}_2$ ,  $100 \mu\text{M}$  ascorbic acid, and  $100 \mu\text{M H}_2\text{O}_2$ ; (d)  $10 \text{ mM NaOCl}$ ; (e)  $0.1 \mu\text{M CuCl}_2$ ,  $100 \mu\text{M}$  ascorbic acid, and  $10 \text{ mM NaOCl}$ ; (f)  $0.1 \mu\text{M CuCl}_2$ ,  $100 \mu\text{M}$  ascorbic acid, and  $2 \text{ mM NaOCl}$ ; and (g)  $0.1 \mu\text{M CuCl}_2$  and  $100 \mu\text{M}$  ascorbic acid.

ascorbic acid and  $100 \mu\text{M H}_2\text{O}_2$  led to a reduction of the dynamic viscosity value to  $5.8 \text{ mPa}\cdot\text{s}$  within  $95 \text{ min}$  (curve c in Figure 1). Yet the oxidative system containing only two reagents,  $0.1 \mu\text{M CuCl}_2$  plus  $100 \mu\text{M}$  ascorbic acid, did not induce the reduction of the dynamic viscosity to  $5.8 \text{ mPa}\cdot\text{s}$  even throughout the entire period of measurement, i.e.,  $300 \text{ min}$  (curve g in Figure 1).

Degradative systems comprising  $\text{NaOCl}$  (cf. curves d, e, and f in Figure 1) caused reduction of the sample dynamic viscosity value: the addition of  $0.1 \mu\text{M CuCl}_2$  along with  $100 \mu\text{M}$  ascorbic acid and  $2 \text{ mM NaOCl}$  resulted in attaining the  $\eta$  value of  $5.8 \text{ mPa}\cdot\text{s}$  within  $221 \text{ min}$  (curve f), whereas  $10 \text{ mM NaOCl}$  alone added to the solution of the LIFECORE P9710-2 sample led to a more rapid decline of the dynamic viscosity (curve d); the magnitude  $\eta = 5.8 \text{ mPa}\cdot\text{s}$  was already reached after  $134 \text{ min}$ . However, as can be seen, the introduction of  $\text{Cu(II)}$ , namely,  $0.1 \mu\text{M CuCl}_2$ , together with  $100 \mu\text{M}$  ascorbic acid and  $10 \text{ mM NaOCl}$  resulted in an extremely fast degradation of the high-molar-mass HA, and the decrease of  $\eta$  value to  $5.8 \text{ mPa}\cdot\text{s}$  was attained within  $12 \text{ min}$  (cf. Figure 1, curve e).

**SEC-MALS.** Table 1 demonstrates the data obtained at the determination of the fragmented polymer molar mass averages (numeric-, weight-, and  $z$ -average,  $M_n$ ,  $M_w$ , and  $M_z$ , respectively), the molar mass corresponding to the peak of the eluted sample in the chromatogram ( $M_p$ ), the dispersity indices ( $M_w/M_n$  and  $M_z/M_w$ ), and the radius of gyration ( $R_g$ ) in  $0.15 \text{ M NaCl}$  solution at  $35^\circ\text{C}$ . As follows from the results presented in Figure 1 and Table 1, the degradative system termed g can be characterized as the less efficient system. The  $M_w$  value of the sample degraded during  $5 \text{ h}$  was  $237.8 \text{ kDa}$  (cf. Table 1). This value resembled the values of  $M_w$  averages of other fragmented polymers. However, it was substantially lower than could be anticipated, on the basis of simple comparison of the observed  $\eta$  values with those of the intact samples LIFECORE P9710-2 and CPN. Thus, it seems feasible to assume that the macromolecules of the LIFECORE P9710-2 sample at a  $0.25\%$  concentration probably form a meshwork, which is able to retain its viscous nature even when the component macromolecules have an  $M_w$  average as low as  $25.1 \text{ kDa}$  (cf. Table 1).



**Table 1.** SEC-MALS Results Obtained with the Fragmented Polymers

sample designation <sup>a</sup>	$M_n$ [kDa]	$M_w$ [kDa]	$M_z$ [kDa]	$M_p$ [kDa]	$M_w/M_n$ [—/—]	$M_z/M_w$ [—/—]	$R_g$ [nm]
HP882	15.5	25.1	39.2	19.1	1.62	1.56	16.1
CU0.1-AA100-HP0.1	111.8	180.4	263.1	161.8	1.61	1.46	37.6
CU0.1-AA100-HOCL2	108.7	166.2	215.5	144.6	1.53	1.30	36.0
CU0.1+AA100	161.7	237.8	323.2	210.5	1.47	1.36	56.2

<sup>a</sup> Codes HP882, CU0.1-AA100-HP0.1, CU0.1-AA100-HOCL2, and CU0.1+AA100 refer to polymer fragments obtained by using degradative systems a, c, f, and g, respectively.

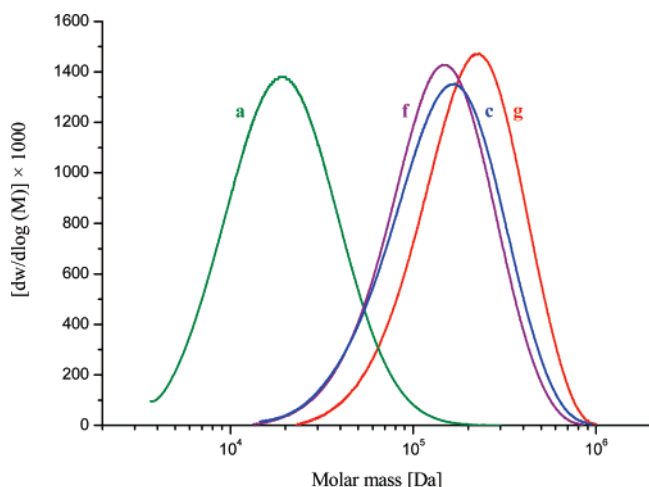
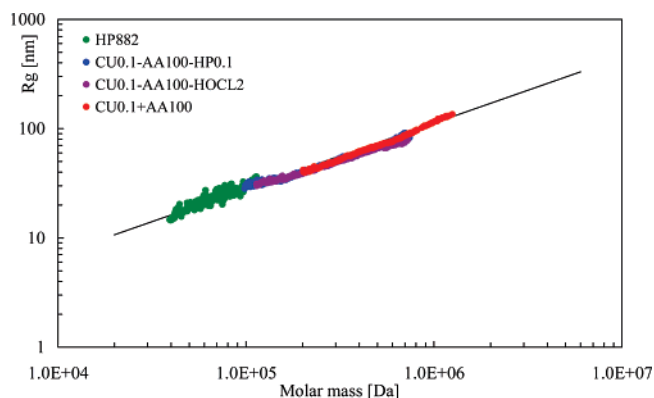
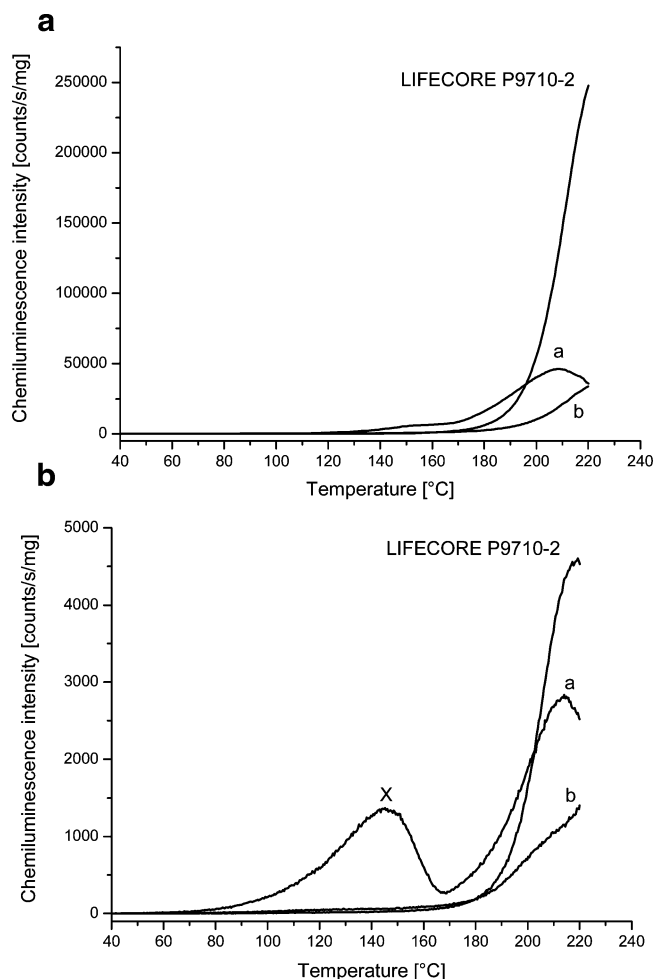
**Figure 2.** Comparison of the differential molar-mass distribution curves of the four polymer fragments degraded by the oxidative systems a, c, f, and g.**Figure 3.** Comparison of the experimental  $R_g = f(M)$  plots of the four polymer fragments.

Figure 2 illustrates differential molar mass distribution of the four polymer fragments determined using the SEC-MALS method. The fact that all fragmented polymers revealed strictly unimodal and symmetrical MMD implies that character/kinetics of the degradation of the LIFECORE P9710-2 sample can be classified as a random process. A very interesting finding is also the relatively low values of the dispersity indices ( $M_w/M_n$ ) ranging from 1.47 to 1.62, which are even lower than the ratio  $M_w/M_n = 1.79$  of the intact LIFECORE P9710-2 sample.

Figure 3 presents a comparison of the experimentally established  $R_g = f(M)$  scaling law, generally known as conformation plot, for the four polymer fragments prepared by using different degradative systems. It is evident that all conformation charts could be described by a single scaling law. As demonstrated in the Figure, the scaling law previously reported for a set of nine HA samples (cf. black line in Figure 3)<sup>25</sup> supports our conclusion that the fragmented polymers in

**Figure 4.** (a) Chemiluminescence intensity. Temperature charts for samples LIFECORE P9710-2 and samples HP882 (a) and CU1.25-HP55 (b) in oxygen. (b) Chemiluminescence intensity. Temperature charts for samples LIFECORE P9710-2 and samples HP882 (a) and CU1.25-HP55 (b) in nitrogen.

solution behave in a manner identical to the behavior of the native HA macromolecules.

**Non-Isothermal Chemiluminometry.** The method monitors the thermal and thermo-oxidation behavior of the intact and fragmented LIFECORE P9710-2 samples. The representative runs for the intact LIFECORE P9710-2 and fragmented samples HP882 and CU1.25-HP55 in oxygen and nitrogen are presented in Figure 4a and b, respectively.

The light emission in oxygen is much more intense than that in nitrogen. It is due to the disproportionation of the peroxy radicals, which are formed as the primary products of the decomposition of the hydroperoxides according to the following reaction:

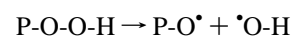
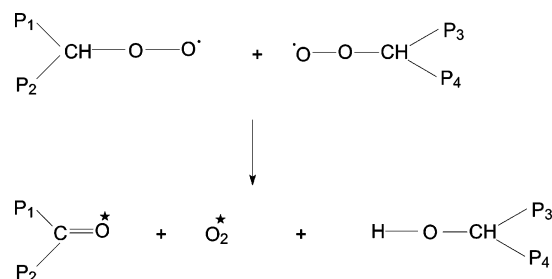


**Table 2.** Rate Constants (in  $\text{s}^{-1}$ ) of Oxidation in Oxygen Determined from Non-Isothermal Chemiluminescence Measurements According to the Previously Described Procedure<sup>27</sup>

sample designation <sup>a</sup>	temperature [°C]		
	40	100	200
LIFECORE P9710-2	$1.1 \times 10^{-9}$	$8.3 \times 10^{-8}$	$2.8 \times 10^{-4}$
HP882	$3.9 \times 10^{-10}$	$1.7 \times 10^{-6}$	$3.9 \times 10^{-4}$
CU1.25-HP55	$5.3 \times 10^{-8}$	$4.7 \times 10^{-6}$	$9.5 \times 10^{-4}$
HOCL10	$1.7 \times 10^{-8}$	$4.0 \times 10^{-7}$	$2.0 \times 10^{-3}$
CU0.1-AA100-HOCL10	$3.7 \times 10^{-8}$	$1.7 \times 10^{-6}$	$1.1 \times 10^{-3}$

<sup>a</sup> Sample codes HP882, CU1.25-HP55, HOCL10, and CU0.1-AA100-HOCL10 relate to HA fragmented by using systems a, b, d, and e, respectively.

The disproportionation occurs as demonstrated in the scheme,



and subsequently, the produced triplet carbonyl and singlet oxygen (denoted with an asterisk) return to their ground state, which is accompanied by the emission of energy (light).<sup>26</sup>

The observation of the high level of the hydroperoxide groups, which remain attached to the HP882 sample, seems to be of high significance. The decomposition of hydroperoxides is reflected by the presence of a distinct peak X (Figure 4b) with a maximum at 140–150 °C. The value of the rate constant of the first-order determined from this peak is  $3.9 \times 10^{-10} \text{ s}^{-1}$  at 40 °C and  $1.7 \times 10^{-6} \text{ s}^{-1}$  at 100 °C (cf. Table 2). This implies that the decomposition of hydroperoxides yielding polymer oxyl radicals and subsequently the scission of the main chain and reduction of the molar mass have taken place. Such decomposition might account for the considerably lower values of the molar mass of sample HP882 established by the SEC-MALS method after some period of time. It can be also stated that the level of hydroperoxides that remains in the sample CU1.25-HP55 is negligible when compared with the sample HP882. The maximum of the molar mass distribution curve is situated at much higher values.

The data in Table 2 provide the average rate constants of oxidation at several selected temperatures. At 40 °C, the highest value for the degraded samples was obtained for the sample CU1.25-HP55 ( $5.3 \times 10^{-8} \text{ s}^{-1}$ ), followed by the sample CU0.1-AA100-HOCL10 ( $3.7 \times 10^{-8} \text{ s}^{-1}$ ), and the sample HOCL10, at which NaOCl alone was applied ( $1.7 \times 10^{-8} \text{ s}^{-1}$ ). The lowest rate constant at 40 °C ( $3.9 \times 10^{-10} \text{ s}^{-1}$ ) was established for the sample HP882. This may be due to the fact that the content of the reactive sites, which may be consumed by oxidation, and which remained after the treatment of the sample LIFECORE P9710-2 was significantly lower in the case of sample HP882 so that the observed rate constant of oxidation was even smaller than that found for the intact HA ( $1.1 \times 10^{-9} \text{ s}^{-1}$ ). Hydroperoxides decompose rather slowly at that temperature. At 100 °C, however, the decomposition of hydroperoxides is faster, and hence, the rate constant of oxidation increases. At higher temperatures such as 200 °C, the lowest stability was found for

the sample HOCL10 (the rate constant  $2.0 \times 10^{-3} \text{ s}^{-1}$ ), followed by the sample prepared by the tri-component mixture CU0.1-AA100-HOCL10 ( $1.1 \times 10^{-3} \text{ s}^{-1}$ ). The lowest values were determined for the two samples, for the preparation of which hydrogen peroxide was applied, namely,  $9.5 \times 10^{-4} \text{ s}^{-1}$  for the CU1.25-HP55 sample and  $3.9 \times 10^{-4} \text{ s}^{-1}$  for sample HP882.

At 200 °C, the values of the rate constants found for all degraded HA samples lay in the range  $3.9 \times 10^{-4} \text{ s}^{-1}$ – $2.0 \times 10^{-3} \text{ s}^{-1}$  and were also higher than the value measured for the intact LIFECORE P9710-2 sample ( $2.8 \times 10^{-4} \text{ s}^{-1}$ ). Hence, it can be concluded that thermal stability of the degraded samples at temperatures above 100 °C is always lower than that of the parent sample.

**MALDI-TOF MS Analysis.** In order to establish which degradation products can be detected in the HA sample treated with the above-mentioned degradative agents, the recovered polymers were also investigated by MALDI-TOF MS. Since native polysaccharides with high molar masses (particularly the acidic ones) cannot be detected by this soft-ionization mass spectrometric method,<sup>24</sup> samples were digested by testicular hyaluronidase prior to analysis. This enzyme is known to produce a mixture of di, tetra, hexa, and octasaccharides, with the largest share of tetrasaccharides.<sup>28</sup>

The MALDI-TOF mass spectra (both positive and negative ion spectra) of the digestion products are shown in Figure 5. It is reported that oligomers of HA are more sensitively detected as negative ions.<sup>23</sup> Although there are some peaks detected at higher  $m/z$  ratios, only the mass region of the tetrasaccharide will be discussed. The molar mass of the (neutral) tetrasaccharide of HA (HA-4) is 776 Da. This calculation assumes the exclusive presence of the free acid, that is, all charges are compensated by  $\text{H}^+$ . Accordingly, the signal at  $m/z$  775.2 corresponds to HA-4 after the loss of one proton, whereas the peak at  $m/z$  797.2 corresponds to the anion of HA-4 following the exchange of one  $\text{H}^+$  by a  $\text{Na}^+$  ion. Independent of the sample treatment, only minor differences between the individual spectra were observed.

The negative ion peaks at  $m/z$  681.0, 641.0, 601.0, and 561.0 as well as at  $m/z$  857.0 and 817.0 stem from the applied matrix (2,5-dihydroxybenzoic acid, with a molar mass of 154 Da) that undergoes oligomerization under the conditions of laser irradiation accompanied by the loss of sodium hydroxide molecules (mass difference of 40 Da).<sup>29</sup> Although all MALDI-TOF MS measurements were performed under identical conditions, it is obvious that the contribution of the matrix signals differs significantly. This is particularly evident when the intensities of the matrix peaks (e.g., at  $m/z$  681.0) are compared with the intensities of the peaks of the HA tetrasaccharide ( $m/z$  775.2 and 797.2). The contribution of matrix peaks is very small in the native HA sample as well as after  $\text{H}_2\text{O}_2$  treatment but is elevated when other degradative systems are used. In the positive ion mode, contribution of the matrix peaks is similar to that observed in the negative ion spectrum.

Very weak peaks appear at  $m/z$  833.3 and 846.3 in the positive ion spectrum, ( $\text{d}_p$ ), after the HOCl treatment. Although the peak at  $m/z$  846.3 cannot be yet assigned, the signal at  $m/z$  833.3 corresponds perfectly to the substitution of  $\text{H}^+$  with  $\text{Cl}^+$ . Nevertheless, because of its low intensity, this peak should not be overestimated.

In the negative ion spectra, the generation of matrix/analyte clusters is also apparent. The mass difference between  $m/z$  973.3 and  $m/z$  775.2 is 198. This corresponds exactly to the molecular mass of DHB after the exchange of two  $\text{H}^+$  with two  $\text{Na}^+$  ions ( $154 \rightarrow 176 \rightarrow 198$ ). This phenomenon has been already

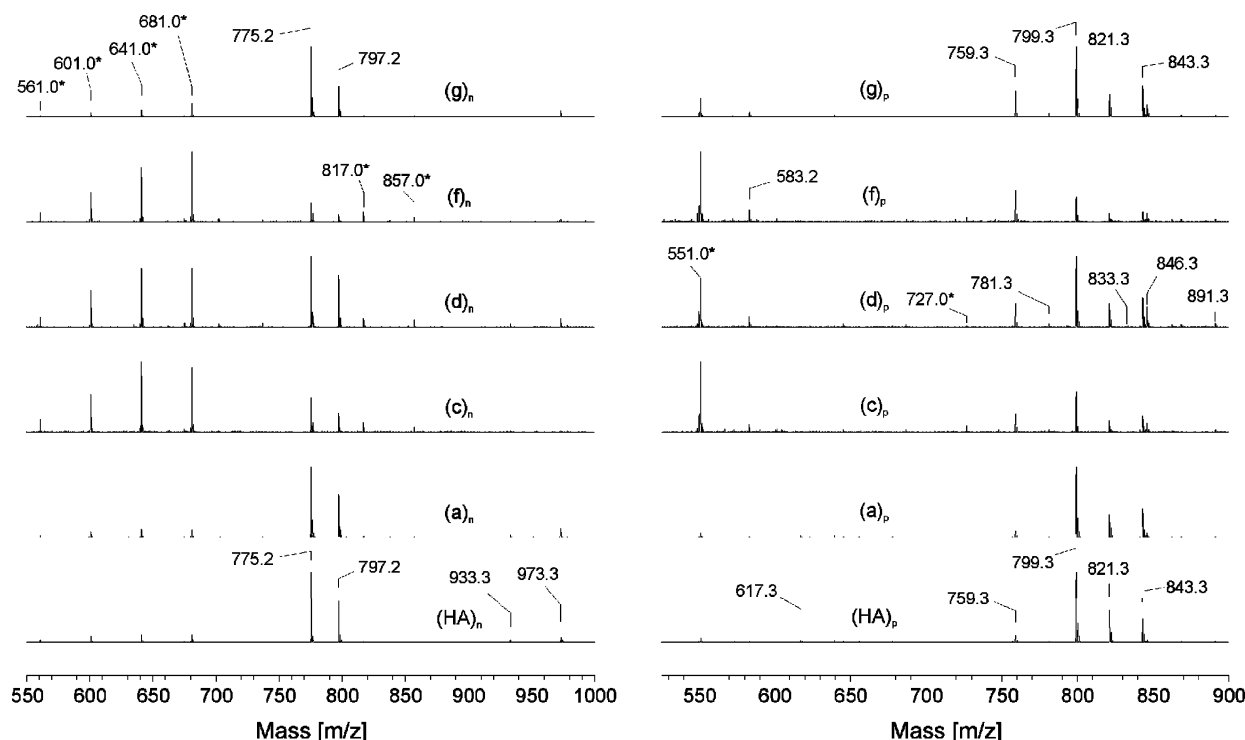


**Figure 5.** Negative (left) and positive (right) ion MALDI-TOF mass spectra of high-molar-mass HA treated with various agents. (HA)<sub>n</sub> and (HA)<sub>p</sub> represent the native sample LIFECORE P9710-2. In (a)<sub>n</sub> and (a)<sub>p</sub>, the native HA sample was treated with 882 mM H<sub>2</sub>O<sub>2</sub>, in (c)<sub>n</sub> and (c)<sub>p</sub> with 0.1  $\mu$ M CuCl<sub>2</sub>, 100  $\mu$ M ascorbic acid and 100  $\mu$ M H<sub>2</sub>O<sub>2</sub>, in (d)<sub>n</sub> and (d)<sub>p</sub> with 10 mM NaOCl, in (f)<sub>n</sub> and (f)<sub>p</sub> with 0.1  $\mu$ M CuCl<sub>2</sub>, 100  $\mu$ M ascorbic acid and 2 mM NaOCl, and in (g)<sub>n</sub> and (g)<sub>p</sub> with 0.1  $\mu$ M CuCl<sub>2</sub> and 100  $\mu$ M ascorbic acid. The peaks are labeled according to their  $m/z$  ratios; the peaks labeled with an asterisk originate from the applied DHB matrix. The indices n and p represent negative and positive ion spectra, respectively.

observed when phospholipids are analyzed; however, it has not been described so far for glycosaminoglycans.<sup>29</sup>

## Discussion

**HA Degradation-Causing Systems.** Hydrogen peroxide, a non-charged non-radical oxidant, does not react with HA. However, traces of transition metals present in HA samples may catalyze the decomposition of H<sub>2</sub>O<sub>2</sub>, resulting in the generation of hydroxyl radicals. The study of the degradative action of various oxidative systems on high-molar-mass HA started at the end of the 1980s has rendered unequivocal proof on the damaging action of the hydroxyl radicals that leads to the reduction of the polymer molar mass and impaired viscoelastic properties of HA.<sup>30–34</sup> The techniques of steady-state and pulse radiolysis were applied to the generation of free radicals, and the formation of  $\bullet$ OH radicals has been proven using EPR spectrometry.

A system containing hydrogen peroxide *plus* cupric cations has been proven to be especially efficient at degrading high-molar-mass HA.<sup>35–38</sup> Recent EPR investigations of H<sub>2</sub>O<sub>2</sub> decomposition by cupric ions (CuCl<sub>2</sub>) using the spin-trapping agent 5,5-dimethyl-1-pyrroline-*N*-oxide (DMPO) have unequivocally corroborated the formation of  $\bullet$ OH radicals.<sup>39</sup> Hence, we may assume that on applying the systems a, b, and c, the ROS that cause the degradation of the HA macromolecule are the  $\bullet$ OH radicals.

Apart from degradative system c involving the direct participation of added H<sub>2</sub>O<sub>2</sub>, it is necessary to emphasize that other degradative systems without H<sub>2</sub>O<sub>2</sub> addition, namely, e, f, and g, could also generate  $\bullet$ OH radicals. A combination of ascorbate *plus* Cu(II) used under aerobic conditions, a so-called Weissberger's system,<sup>40,41</sup> gives rise to H<sub>2</sub>O<sub>2</sub>,<sup>42–44</sup> and taking into

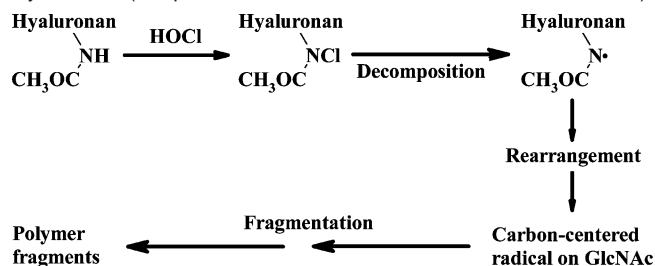
account the fact that ascorbate reduces Cu(II) to cuprous ions, it is feasible to assume that systems e, f, and g degrade HA macromolecules by the action of  $\bullet$ OH radicals. This conclusion is supported by an unambiguous proof of the production of hydroxyl radicals in a system comprising ascorbate *plus* CuCl<sub>2</sub> obtained by using an EPR spin-trap technique applying such spin traps as DMPO and 5-(diisopropoxyphosphoryl)-5-methyl-1-pyrroline-*N*-oxide (DIPPMPO).<sup>45</sup>

The only system that degrades HA macromolecules and lacks H<sub>2</sub>O<sub>2</sub> is system d, that is, 10 mM HOCl/OCl<sup>–</sup>. However, under *in vivo* conditions, the generation of millimolar concentrations of hypochlorite looks unrealistic. HOCl concentrations of the order of 340  $\mu$ M were reported to be of relevance in the inflamed joint;<sup>46</sup> however, its quantitative assay under *in vivo* conditions is extremely difficult because of the large number of reactive molecules present. In fact, the question of which HOCl concentrations are relevant is a very complicated issue because recently, it has been postulated that HOCl may occur *in vivo* in 100 mM and even higher concentrations.<sup>47</sup>

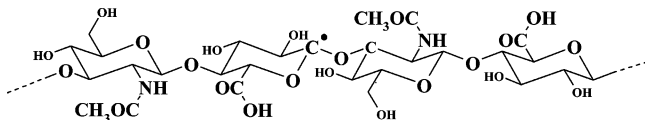
Here, it would be appropriate to emphasize that HOCl reacts with chloride anions generating active chlorine in agreement with the following reaction: HOCl + Cl<sup>–</sup>  $\leftrightarrow$  Cl<sub>2</sub> + HO<sup>–</sup>. Hence, applying the systems d, e, and f, a direct reaction between the functional groups on the HA macromolecule and Cl<sub>2</sub> should also be taken into consideration.

**Chemistry of ROS Attack of the HA Macromolecule.** In the aqueous milieu, the hydroxyl radical represents the most reactive species. It reacts with virtually all compounds containing C–H groups, abstracting the hydrogen radical (H $\bullet$ ) and leading to the generation of the corresponding C-centered radical. In the case of the HA macromolecule, while  $\bullet$ OH attack of the glucuronic acid unit occurs randomly at all sites of the carbon ring, the *N*-acetylglucosamine moiety is attacked more

**Scheme 1.** Outline of Events that May Occur on Reaction of HOCl with the *N*-Acetylglucosamine (GlcNAc) Moiety of Hyaluronan (Adapted with Permission from Hawkins and Davies<sup>51</sup>)

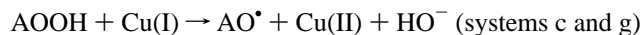


specifically. No radicals are formed at the C-2 or methyl carbon of the acetyl group.<sup>48</sup> The resulting C-centered radical is



hereafter referred to simply as A•.

Subsequently, the radical A• traps one molecule of oxygen yielding AOO•, which can naturally participate in the reactions leading to further production of A• (AOO• + HA → AOOH + A•). Then, because of the AOOH decomposition catalyzed by cuprous ions maintained in a lower oxidation state by ascorbate,

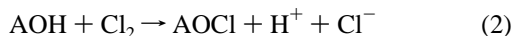


the generated AO• radicals can undergo a  $\beta$ -scission, yielding polymer fragments with reduced molar mass.<sup>49</sup>

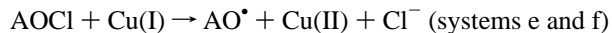
Hydroxyl radicals may also affect the d-glucuronate/d-glucuronic acid units or *N*-acetylglucosamine moieties of HA leading to the opening of the pyranose ring(s) without cleaving the polymer chain.<sup>48</sup> However, subsequent radical reactions or rearrangement of the generated C-centered radicals may produce polymer fragments of even lower molar mass.

Rees et al.<sup>50</sup> demonstrate that the reaction of HOCl with the *N*-acetyl group of *N*-acetylglucosamine moieties of HA leads to the formation of long-lived *N*-chloroamides (cf. Scheme 1). The reaction continues with the production of *N*-centered amidyl radicals, which isomerize, rendering carbon-centered radicals at C-2 of the *N*-acetylglucosamine units and at C-4 of the neighboring uronic acid residues. The C-4 carbon-centered radicals subsequently undergo  $\beta$ -scission reactions that result in glycosidic bond cleavage, which yields polymer fragments of lower molar mass.

Recently, another possible pathway has been proposed:<sup>49</sup> hydroxyl group(s) on HA (denoted AOH) might react directly with both HOCl and Cl<sub>2</sub> according to the following reactions:



The intermediate HA hypochlorite (AOCl) decomposes readily under the catalytic action of cuprous ions maintained in a lower oxidation state by ascorbate.



The AO• radical undergoes fragmentation, which results in the production of polymer fragments with reduced molar mass.

The incorporation of a Cl atom into the HA polymer chain by reactions 1 and/or 2 and/or the reactions depicted in Scheme

1 is supported particularly well by the results obtained by MALDI-TOF MS analyses of the polymer fragments, which were obtained upon treatment of HA with system d, that is, with 10 mM NaOCl. However, these mass spectrometric data do not permit to unambiguously conclude, whether N-H is converted into N-Cl or OH into OCl. Kinetic reference data indicate a much higher reactivity of the glucosamine unit in comparison to that of glucuronic acid.<sup>52</sup> Accordingly, the generation of *N*-chloroamide seems to be a more probable pathway.

**Biological Consequences.** A 3% solution of hydrogen peroxide (ca. 882 mM) is routinely used, for example, for the disinfection of superficial wounds. Taking into consideration the omnipresent occurrence of traces of (transition) metal ions, it can be assumed that hydroxyl radicals generated from H<sub>2</sub>O<sub>2</sub> may degrade HA macromolecules within the epidermis either directly or via stimulating HA catabolism by keratinocytes.<sup>53,54</sup> Even much lower concentrations of H<sub>2</sub>O<sub>2</sub> are very efficient regarding the degradation of HA macromolecules in the presence of micro- or submicromolar concentrations of transition metal ions independently from the presence of (physiological) concentration of ascorbate. As can be seen from the results presented in Figure 1 and Table 1, degradative systems a, b, and c can cause the decline of *M<sub>w</sub>* from an initial value of 1.2 MDa to the values 1 or 2 orders lower within a relatively short time period. Bearing in mind that intermediate-sized HA fragments have angiogenic and immunostimulating properties, it would be advisable to assess polymeric materials prepared by treating high-molar-mass HA with degrading systems a, b, or c for their potential effects on topical application in the treatment of burn injuries.

Degradative systems d, e, and f with their qualitative composition mimic to a certain extent the situation occurring under inflammatory conditions in which the heme enzyme myeloperoxidase (MPO) released from activated neutrophils generates hypochlorous acid from H<sub>2</sub>O<sub>2</sub> molecules. However, as documented by the results of this study as well as by previous observations,<sup>50–51,55–57</sup> fragmentation of HA macromolecules required the presence of at least millimolar concentrations of HOCl.

Oxidative system g is unique in its composition from several viewpoints: (i) under physio as well as pathophysiological/inflammatory conditions, a co-operation of submicromolar concentrations of copper ions and tens/hundreds of micromolar ascorbate concentrations can be assumed; (ii) ascorbate with the catalytic assistance of copper ions transforms molecular oxygen directly to hydrogen peroxide; (iii) ascorbate is able to reduce Cu(II) to cuprous ions and in this way confers the possibility to generate •OH radicals by a Fenton-type reaction: Cu(I) + H<sub>2</sub>O<sub>2</sub> → Cu(II) + •OH + HO<sup>–</sup>; (iv) ascorbate scavenges •OH radicals while turning into a non-radical product, dehydroascorbate. As has been shown in many studies, under aerobic conditions, a ternary system comprising HA macromolecules plus ascorbate and the traces of transition metal ions (mostly iron or copper) reveals a gradual decrease of the viscosity of the HA solution as a result of the fragmentation/degradation of HA macromolecules. For this reason, polymer fragments prepared by applying oxidative system g should be considered a prime candidate for the assessment of their angiogenic, pro-inflammatory, and immunostimulating properties. The polymer fragments prepared in this way are closely related to those intermediate- and/or small-sized HA fragments that are produced during physiological/pathophysiological HA catabolism/degradation.



### Concluding Remarks

As described in our recent overview, oxidizing agents of different origins may lead to various changes in the structure of the rather susceptible biopolymer, HA.<sup>58</sup> The importance of the information carried by different size-specific HA fragments and subsequently mediated to various cells in the human organism is generally recognized.<sup>59</sup> It is thus feasible that changes introduced to the HA structure by the fragmentation technique applied to manufacturing commercially available HA preparations such as the possible presence of peroxide, carbonyl, carboxyl, or other exogenous substituents might represent an unknown risk factor that could be manifested upon therapeutic application in humans. Therefore, it would be advisable for manufacturers to provide in the product specification the description of the fragmentation techniques applied for producing HA of lower molar mass as well as the assessment of chemical modification of the HA structure. Without such prior information, the consequences of the administration of insufficiently characterized HA preparations in human therapy could be potentially harmful.

**Acknowledgment.** The grants VEGA 2/5002/05, 2/7028/27, 2/7033/7, and APVT 99-P03305 as well as APVV 51-017905 are gratefully acknowledged. This work was also supported by the German Research Council (DFG Schi 476/5-1) and the German Federal Ministry of Education and Research (Grant BMBF 0313836). The kind gift of the hyaluronan sample from Dr. K. Thacker is much appreciated.

### References and Notes

- Itano, N.; Sawai, T.; Yoshida, M.; Lenas, P.; Yamada, Y.; Imagawa, M.; Shinomura, T.; Hamaguchi, M.; Yoshida, Y.; Ohnuki, Y.; Miyauchi, S.; Spicer, A. P.; McDonald, J. A.; Kimata, K. Three isoforms of mammalian hyaluronan synthases have distinct enzymatic properties. *J. Biol. Chem.* **1999**, *274*, 25085–25092.
- Chong, B. F.; Blank, L. M.; McLaughlin, R.; Nielsen, L. Microbial hyaluronan production. *Appl. Microbiol. Biotechnol.* **2005**, *66*, 341–351.
- Tranchepain, F.; Deschrevel, B.; Courel, M.-N.; Levasseur, N.; Le Cerf, D.; Loutelier-Bourhis, C.; Vincent, J.-C. A complete set of hyaluronan fragments obtained from hydrolysis catalyzed by hyaluronidase: Application to studies of hyaluronan mass distribution by simple HPLC devices. *Anal. Biochem.* **2006**, *348*, 232–242.
- Capila, I.; Sasisekharan, R. Methods for Analysis of Hyaluronan and Its Fragments. In *Chemistry and Biology of Hyaluronan*; Garg, H. G., Hales, C. A., Eds.; Elsevier Press: Amsterdam, The Netherlands, 2004; pp 21–40.
- Feinberg, R. N.; Beebe, D. C. Hyaluronate in vasculogenesis. *Science* **1983**, *220*, 1177–1179.
- McBride, W. H.; Bard, J. B. Hyaluronidase-sensitive halos around adherent cells. Their role in blocking lymphocyte-mediated cytotoxicity. *J. Exp. Med.* **1979**, *149*, 507–515.
- Delmage, J. M.; Powars, D. R.; Jaynes, P. K.; Allerton, S. E. The selective suppression of immunogenicity by hyaluronan. *Ann. Clin. Lab. Sci.* **1986**, *16*, 303–310.
- Noble, P. W. Hyaluronan and its catabolic products in tissue injury and repair. *Matrix Biol.* **2002**, *21*, 25–29.
- West, D. C.; Hampson, I. N.; Arnold, F.; Kumar, S. Angiogenesis induced by degradation products of hyaluronan. *Science* **1985**, *228*, 1324–1326.
- Hyalose, L.L.C. <http://www.hyalose.com>.
- Schiller, J.; Fuchs, B.; Arnold, K. The molecular organization of polymers of cartilage: An overview of health and disease. *Curr. Org. Chem.* **2006**, *10*, 1771–1789.
- Šoltés, L.; Stankovská, M.; Kogan, G.; Gemeiner, P.; Stern, R. Contribution of oxidative-reductive reactions to high-molecular-weight hyaluronan catabolism. *Chem. Biodiversity* **2005**, *2*, 1242–1245.
- Moseley, R.; Waddington, R. J.; Embury, G. Degradation of glycosaminoglycans by reactive oxygen species derived from stimulated polymorphonuclear leukocytes. *Biochim. Biophys. Acta* **1997**, *1362*, 221–231.
- Stankovská, M.; Šoltés, L.; Vikartovská, A.; Mendichi, R.; Lath, D.; Molnárová, M.; Gemeiner, P. Study of hyaluronan degradation by means of rotational viscometry: Contribution of the material of viscometer. *Chem. Pap.* **2004**, *58*, 348–352.
- Ullrich, O.; Reinheckel, T.; Sitte, N.; Grune, T. Degradation of hypochlorite-damaged glucose-6-phosphate dehydrogenase by the 20S proteasome. *Free Radical Biol. Med.* **1999**, *27*, 487–492.
- Banerjee, D.; Kumar, P. A.; Kumar, B.; Madhusoodanan, U. K.; Nayak, S.; Jacob, J. Determination of absolute hydrogen peroxide concentration by spectrophotometric method. *Curr. Sci.* **2002**, *83*, 1193–1194.
- Morris, J. C. The acid ionization constant of HOCl from 5 to 35. *J. Phys. Chem.* **1966**, *70*, 3798–3805.
- Stankovská, M.; Šoltés, L.; Vikartovská, A.; Gemeiner, P.; Kogan, G.; Bakoš, D. Degradation of high-molecular-weight hyaluronan: a rotational viscometry study. *Biologia* **2005**, *60* (Suppl. 17), 149–152.
- Wyatt, P. J. Light-scattering and the absolute characterization of macromolecules. *Anal. Chim. Acta* **1993**, *272*, 1–40.
- Mendichi, R.; Giacometti Schieroni, A.; Grassi, C.; Re, A. Characterization of ultra-high molar mass hyaluronan: 1. Off-line static methods. *Polymer* **1998**, *39*, 6611–6620.
- Mendichi, R.; Giacometti Schieroni, A. Fractionation and characterization of ultra-high molar mass hyaluronan: 2. On-line size exclusion chromatography methods. *Polymer* **2002**, *43*, 6115–6121.
- Hao, C.; Ma, X.; Fang, S.; Liu, Z.; Liu, S.; Song, F.; Liu, J. Positive- and negative-ion matrix-assisted laser desorption/ionization mass spectrometry of saccharides. *Rapid Commun. Mass Spectrom.* **1998**, *12*, 345–348.
- Busse, K.; Averbeck, M.; Anderegg, U.; Arnold, K.; Simon, J. C.; Schiller, J. The signal-to-noise ratio as a measure of HA oligomer concentration: a MALDI-TOF MS study. *Carbohydr. Res.* **2006**, *341*, 1065–1070.
- Schiller, J.; Arnold, K. Mass Spectrometry in Structural Biology. In *Encyclopedia of Analytical Chemistry*; Meyers, R. A., Ed.; John Wiley & Sons Ltd.: Chichester, England, 2000; pp 559–568.
- Mendichi, R.; Šoltés, L.; Giacometti-Schieroni, A. Evaluation of radius of gyration and intrinsic viscosity molar mass dependence and stiffness of hyaluronan. *Biomacromolecules* **2003**, *4*, 1805–1810.
- Jacobsson, K.; Eriksson, P.; Reitberger, T.; Stenberg, B. Chemiluminescence as a tool for polyolefin oxidation studies. *Adv. Polym. Sci.* **2004**, *169*, 151–176.
- Rychlý, J.; Strlič, M.; Matisová-Rychlá, L.; Kolar, J. Chemiluminescence from paper. Kinetic analysis of thermal oxidation of cellulose. *Polym. Degrad. Stab.* **2002**, *78*, 357–367.
- Schiller, J.; Arnhold, J.; Benard, S.; Reichl, S.; Arnold, K. Cartilage degradation by hyaluronate lyase and chondroitin ABC lyase: a MALDI-TOF mass spectrometric study. *Carbohydr. Res.* **1999**, *318*, 116–122.
- Schiller, J.; Süß, R.; Fuchs, B.; Müller, M.; Petkovic, M.; Zschörnig, O.; Waschpky, H. The suitability of different DHB isomers as matrices for the MALDI-TOF MS analysis of phospholipids: which isomer for what purpose? *Eur. Biophys. J.* **2007**, *36*, 517–527.
- Deeble, D. J.; Bothe, E.; Schuchmann, H. P.; Parsons, B. J.; Phillips, G. O.; von Sonntag, C. The kinetics of hydroxyl-radical-induced strand breakage of hyaluronan. A pulse radiolysis study using conductometry and laser-light-scattering. *Z. Naturforsch., C: J. Biosci.* **1990**, *45*, 1031–1043.
- Parsons, B. J.; Al-Assaf, S.; Navaratnam, S.; Phillips, G. O. Comparison of the Reactivity of Different Oxidative Species (ROS) towards Hyaluronan. In *Hyaluronan. Chemical, Biochemical and Biological Aspects*; Kennedy, J. F., Phillips, G. O., Williams, P. A., Eds.; Hascall, V. C., Guest Ed.; Woodhead Publishing Ltd.: Cambridge, England, 2002; Vol. 1, pp 141–150.
- Myint, P.; Deeble, D. J.; Beaumont, P. C.; Blake, S. M.; Phillips, G. O. The reactivity of various free radicals with hyaluronan: steady-state and pulse radiolysis studies. *Biochim. Biophys. Acta* **1987**, *925*, 194–202.
- Al-Assaf, S.; Meadows, J.; Phillips, G. O.; Williams, P. A.; Parsons, B. J. The effect of hydroxyl radicals on the rheological performance of hyaluronan and hyaluronan. *Int. J. Biol. Macromol.* **2000**, *27*, 337–348.
- Al-Assaf, S.; Hawkins, C. L.; Parsons, B. J.; Davies, M. J.; Phillips, G. O. Identification of radicals from hyaluronan (hyaluronic acid) and cross-linked derivatives using electron paramagnetic resonance spectroscopy. *Carbohydr. Polym.* **1999**, *38*, 17–22.

- (35) Deeble, D. J.; Parsons, B. J.; Phillips, G. O.; Myint, P.; Beaumont, P. C.; Blake, S. M. Influence of Copper Ions on Hyaluronic Acid Free Radical Chemistry. In *Free Radical Metal Ions and Biopolymers*; Beaumont, P. C., Deeble, D. J., Parsons, B. J., Rice-Evans, C., Eds.; Richelieu Press: London, 1989; pp 159–182.
- (36) Li, M.; Rosenfeld, L.; Vilar, R. E.; Cowman, M. K. Degradation of hyaluronan by peroxynitrite. *Arch. Biochem. Biophys.* **1997**, *341*, 245–250.
- (37) Orviský, E.; Šoltés, L.; Stančíková, M. High-molecular-weight hyaluronan: a valuable tool in testing the antioxidative activity of amphiphilic drugs stobadine and vinpocetine. *J. Pharm. Biomed. Anal.* **1997**, *16*, 419–424.
- (38) Šoltés, L.; Lath, D.; Mendichi, R.; Bystrický, P. Radical degradation of high molecular weight hyaluronan: Inhibition of the reaction by ibuprofen enantiomers. *Methods Find. Exp. Clin. Pharmacol.* **2001**, *23*, 65–71.
- (39) Šoltés, L.; Brezová, V.; Stankovská, M.; Kogan, G.; Gemeiner, P. Degradation of high-molecular-weight hyaluronan by hydrogen peroxide in the presence of cupric ions. *Carbohydr. Res.* **2006**, *341*, 639–644.
- (40) Weissberger, A.; LuValle, J. E.; Thomas, D. S., Jr. Oxidation processes. XVI. The autoxidation of ascorbic acid. *J. Am. Chem. Soc.* **1943**, *65*, 1934–1939.
- (41) Khan, M. M.; Martell, A. E. Metal ion and metal chelate catalyzed oxidation of ascorbic acid by molecular oxygen. I. Cupric and ferric ion catalyzed oxidation. *J. Am. Chem. Soc.* **1967**, *89*, 4176–4185.
- (42) Fisher, A. E.; Naughton, D. P. Vitamin C contributes to inflammation via radical generating mechanisms: a cautionary note. *Med. Hypotheses* **2003**, *61*, 657–660.
- (43) Fisher, A. E. O.; Naughton, D. P. Iron supplements: the quick fix with long-term consequences. *Nutrition J.* **2004**, *3*, 1–5.
- (44) Fisher, A. E. O.; Naughton, D. P. Therapeutic chelators for the twenty first century: new treatments for iron and copper mediated inflammatory and neurological disorders. *Curr. Drug Delivery* **2005**, *2*, 261–268.
- (45) Šoltés, L.; Stankovská, M.; Brezová, V.; Schiller, J.; Arnhold, J.; Kogan, G.; Gemeiner, P. Hyaluronan degradation by copper(II) chloride and ascorbate: rotational viscometric, EPR spin-trapping, and MALDI-TOF mass spectrometric investigations. *Carbohydr. Res.* **2006**, *341*, 2826–2834.
- (46) Katrantzis, M.; Baker, M. S.; Handley, C. J.; Lowther, D. A. The oxidant hypochlorite ( $\text{OCl}^-$ ), a product of the myeloperoxidase system, degrades articular cartilage proteoglycan aggregate. *Free Radical Biol. Med.* **1991**, *10*, 101–109.
- (47) Winterbourn, C. C.; Hampton, M. B.; Livesey, J. H.; Kettle, A. J. Modeling the reactions of superoxide and myeloperoxidase in the neutrophil phagosome: implications for microbial killing. *J. Biol. Chem.* **2006**, *281*, 39860–39869.
- (48) Hawkins, C. L.; Davies, M. J. Direct detection and identification of radicals generated during the hydroxyl-induced degradation of hyaluronic acid and related materials. *Free Radical Biol. Med.* **1996**, *21*, 275–290.
- (49) Rychlý, J.; Šoltés, L.; Stankovská, M.; Janigová, I.; Csomorová, K.; Sasinková, V.; Kogan, G.; Gemeiner, P. Unexplored capabilities of chemiluminescence and thermoanalytical methods in characterization of intact and degraded hyaluronans. *Polym. Degrad. Stab.* **2006**, *91*, 3174–3184.
- (50) Rees, M. D.; Hawkins, C. L.; Davies, M. J. Hypochlorite-mediated fragmentation of hyaluronan, chondroitin sulfates, and related *N*-acetyl glycosamines: evidence for chloramide intermediates, free radical transfer reactions, and site-specific fragmentation. *J. Am. Chem. Soc.* **2003**, *125*, 13719–13733.
- (51) Hawkins, C. L.; Davies, M. J. Degradation of hyaluronic acid, poly and mono-saccharides, and model compounds by hypochlorite: Evidence for radical intermediates and fragmentation. *Free Radical Biol. Med.* **1998**, *24*, 1396–1410.
- (52) Rees, M. D.; Pattison, D. I.; Davies, M. J. Oxidation of heparan sulphate by hypochlorite: role of *N*-chloro derivatives and dichloramine-dependent fragmentation. *Biochem. J.* **2005**, *391*, 125–134.
- (53) Tammi, R.; Saamanen, A.-M.; Maibach, H. I.; Tammi, M. Degradation of newly synthesized high molecular mass hyaluronan in the epidermal and dermal compartments of human skin in organ culture. *J. Invest. Dermatol.* **1991**, *97*, 126–130.
- (54) Agren, U. M.; Tammi, R. H.; Tammi, M. I. Reactive oxygen species contribute to epidermal hyaluronan catabolism in human skin organ culture. *Free Radical Biol. Med.* **1997**, *23*, 996–1001.
- (55) Baker, M. S.; Green, S. P.; Lowther, D. A. Changes in the viscosity of hyaluronic acid after exposure to a myeloperoxidase-derived oxidant. *Arthritis Rheum.* **1989**, *32*, 461–467.
- (56) Jahn, M.; Baynes, J. W.; Spiteller, G. The reaction of hyaluronic acid and its monomers, glucuronic acid and *N*-acetylglucosamine, with reactive oxygen species. *Carbohydr. Res.* **1999**, *321*, 228–234.
- (57) Rees, M. D.; Hawkins, C. L.; Davies, M. J. Hypochlorite and superoxide radicals can act synergistically to induce fragmentation of hyaluronan and chondroitin sulphate. *Biochem. J.* **2004**, *381*, 175–184.
- (58) Šoltés, L.; Mendichi, R.; Kogan, G.; Schiller, J.; Stankovská, M.; Arnhold, J. Degradative action of reactive oxygen species on hyaluronan. *Biomacromolecules* **2006**, *7*, 659–668.
- (59) Stern, R.; Asari, A. A.; Sugahara, K. N. Hyaluronan fragments: An information-rich system. *Eur. J. Cell. Biol.* **2006**, *85*, 699–715.

BM070309B